



# Synchrotron infrared microspectroscopic analysis of collagens I, III, and elastin on the shoulders of human thin-cap fibroatheromas

David L. Wetzel<sup>a,\*</sup>, Ginell R. Post<sup>b</sup>, Robert A. Lodder<sup>c</sup>

<sup>a</sup> Microbeam Molecular Spectroscopy Laboratory, Kansas State University, Shellenberger Hall, Manhattan, KS 66506-2201, USA

<sup>b</sup> Department of Pathology and Laboratory Medicine, College of Medicine, University of Kentucky, Lexington, KY 40506-0082 USA

<sup>c</sup> Chemistry Department, University of Kentucky, Lexington, KY 40506-0886, USA

Accepted 14 February 2005

## Abstract

Of the many people who experience a sudden cardiac event (acute coronary syndromes and/or sudden cardiac death), a large portion has no prior symptoms. One potential *in vivo* spectroscopic technique for diagnosis of pathological conditions that underlie these sudden cardiac events involves the use of a near-infrared spectrometric catheter with moderate *in vivo* spatial resolution. To justify the time and expense of such an *in vivo* protocol, the putative vulnerable narrow region at the shoulder of the thin cap fibroatheroma is chemically characterized by high spatial resolution mid-infrared microspectroscopy. The sharp peaks of the mid-infrared and the previous band assignments that are readily available are useful in establishing the basis needed to support the development and validity of future *in vivo* NIR probing. The spatial resolution of *in vivo* NIR spectrometric catheters is limited by light scattering from blood and by the motion of the catheter and blood vessel wall, making it difficult to characterize a fibrous cap in the rupture zone. However, the spatial resolution of *in vitro* synchrotron IR microspectroscopy is high and probably sufficient to characterize chemically the actual area of disruption. A thin-cap fibroatheroma is a rupture-prone plaque. The shoulder of the cap (where the cap meets the vessel wall) is most vulnerable to rupture because mechanical stress at this point weakens the collagen and elastin fibers. It is hypothesized that the breakdown of elastin is highest in this target zone, followed by collagen III. The analysis of collagen I, collagen III, and elastin concentration in the small (ca. 10  $\mu\text{m}$ ) interface zone, between the intimal wall of the artery and the fibrous cap, is of concern because it is the shoulder where the protein degradation is expected to be the highest. (A similar degradation occurs on a larger scale in the vessel wall in abdominal aortic aneurysm.) For this reason, if confirmed, testing at this location would presumably offer the highest sensitivity and provide the earliest possible warning of rupture-prone plaque. In the current study, post-mortem human tissue was used. Future experiments will be performed on animal models where *in vivo* NIR catheterization is followed by post-mortem mid-infrared microspectroscopy on the same animal. Subsequently it may be possible to develop *in vivo* near-infrared spectrometric catheter techniques suitable for use with human subjects in a clinical setting.

© 2004 Elsevier B.V. All rights reserved.

**Keywords:** Collagens; Human; Fibroatheromas

## 1. Introduction

Cardiovascular disease has been the primary cause of death in industrialized countries for some time, and it is rapidly becoming the number one killer in the developing countries [1]. According to recent estimates, 61,800,000 Americans have one or more types of cardiovascular disease.

Each year, more than 1 million people in the United States and more than 19 million others worldwide suffer a sudden cardiac event (acute coronary syndromes and/or sudden cardiac death). A considerable segment of this population has no preceding symptom. There is a mandate for diagnosis and treatment of the pathologic conditions that lie beneath these sudden cardiac events, and identifying vulnerable plaques and patients.

The word “vulnerable” is used to denote the probability of exhibiting an event in the future. The word vulnerable has

\* Corresponding author.

E-mail address: dlw@wheat.ksu.edu (D.L. Wetzel).

52 been employed in a variety of reports in the medical  
53 literature, all of which portray conditions predisposed to  
54 injury. In this respect, the term “vulnerable plaque” is most  
55 appropriate to classify plaques susceptible to complications.  
56 In contrast, interventional cardiologists and cardiovascular  
57 pathologists retrospectively explain the plaque responsible  
58 for coronary occlusion and death as a culprit plaque, apart  
59 from its histopathologic appearance. However, for prospec-  
60 tive evaluation, diagnosis, and treatment, clinicians require a  
61 term like culprit for identifying such plaques before an event  
62 occurs.

63 Plaque rupture is the most frequent type of plaque  
64 complication, accounting for in excess of 70% of fatal  
65 acute myocardial infarctions and/or sudden coronary  
66 deaths. A number of retrospective autopsy series and a  
67 handful of cross-sectional clinical studies have indicated  
68 that thrombotic coronary death and acute coronary  
69 syndromes are instigated by plaque features and associated  
70 factors. The majority of methods for detecting and treating  
71 vulnerable plaque are dedicated to rupture-prone plaque.  
72 This class of plaque is commonly called a “thin-cap  
73 fibroatheroma”.

74 A thin-cap fibroatheroma is typified by a large lipid core  
75 rich in cholesterol and cholesterol esters. These plaques have  
76 a cap thickness of less than 100  $\mu\text{m}$  and a lipid core  
77 accounting for greater than 40% of the plaque’s total volume  
78 [2]. Potential *in vivo* intravascular diagnostic techniques  
79 include optical coherence tomography (OCT), intravascular  
80 ultrasonography (IVUS), elastography (palpography), MRI,  
81 angiography, and near-infrared spectroscopy. Increasing  
82 evidence substantiates that diverse types of vulnerable  
83 plaque with differing histopathology and biology exist.  
84 Autopsy [3] and IVUS studies [4] have demonstrated that  
85 atherosclerotic lesions commonly exist in young and  
86 asymptomatic persons. The percentage of these lesions that  
87 represent morphologies of rupture-prone vulnerable plaques  
88 remains to be determined. Furthermore, chronic inflamma-  
89 tion [5] and macrophage/foam cell formation are a  
90 fundamental element of the natural history of atherosclero-  
91 sis. To assess plaque vulnerability, it is apparent that a  
92 collective methodology able to appraise structural char-  
93 acteristics (morphology) as well as functional properties  
94 (activity) of plaque will likely be most revealing, and may  
95 offer higher prognostic value than a single method.

96 Among the first changes in the arterial wall in  
97 atherosclerosis is an increase in retained lipoproteins and  
98 ensuing oxidation in the subendothelial matrix [5]. Develop-  
99 ment of lipid-laden macrophages (foam cells) is another  
100 characteristic of the early atherosclerotic progression.  
101 Proliferation and phenotypic alterations in smooth muscle  
102 cells are also observed. The highly developed atherosclero-  
103 tic lesion may be distinguished by amassing of extracellular  
104 lipid, growth of a lipid-rich necrotic core, establishment of a  
105 fibrous cap, and calcification. Atherosclerosis in the arterial  
106 wall is associated with aneurysm, although it is not clear that  
107 this is an underling contributory relationship.

Abdominal aortic aneurysms (AAAs) are potentially life- 108  
threatening conditions that arise in up to 10% of the elderly 109  
populations in industrialized nations. Similar fibrous protein 110  
composition changes have been observed in both the plaque 111  
cap in atherosclerosis and in the media and adventitia of 112  
AAAs. However, an aneurysm is roughly defined as a 113  
permanent dilatation of an artery limited to a small area. 114  
AAAs occur due to considerable remodeling of the 115  
extracellular matrix and are regularly accompanied by 116  
atherosclerosis. They may be manifested by catastrophic 117  
rupture, markers of pressure on other viscera, or an 118  
embolism initiating in the aneurysm wall, but most are 119  
asymptomatic. Collagen and elastin are the main structural 120  
components of vessel walls that have been broadly 121  
implicated in aneurysm formation, progression, and rupture. 122  
These same proteins are found in the cap of fibroatheromas. 123  
The prevailing structural modification linked with human 124  
AAAs that has been reported is a loss in elastin 125  
concentration in the aortic wall. Significant correlations 126  
between lowering elastin concentration and increasing AAA 127  
diameter have been noted. One proposed mechanism for 128  
reduced elastin concentrations is degradation or loss brought 129  
about by elastolysis. Although there have been differences in 130  
the findings of many studies, it is clear that increases in the 131  
collagen-to-elastin ratio are a universal observation in 132  
AAAs. Analytical methods capable of analyzing collagen 133  
and elastin content of arteries *in vivo* could be valuable in the 134  
diagnosis of aneurysm and atherosclerosis, and might even 135  
permit prediction of future clinical events. 136

Diffuse reflection near-infrared spectroscopy has proven 137  
to be a useful technique for identifying chemical content of 138  
atherosclerotic tissues [7]. Our laboratory has described the 139  
use of near-IR spectroscopy to categorize human aortic 140  
atherosclerotic plaques and to quantify cholesterol, HDL, 141  
and LDL in arterial wall samples [8,9]. In a previously study 142  
[6], our laboratory also published the near-infrared spectra 143  
of collagen I, III, and elastin. The collagens and elastin 144  
possess distinctive near-IR spectra that permit identification 145  
and quantification in tissue samples. The data presented in 146  
this report show that collagen I, III, and elastin also have 147  
distinctive mid-infrared spectra. While the precise relation- 148  
ship between mid-IR fundamental signals and near-IR 149  
overtone and combination signals is not always clear, the 150  
fact that these target analytes are distinguishable in both 151  
spectral regions increases the likelihood that clinical 152  
observations made in the IR *in vitro* will translate into 153  
some form that is useful diagnostically in the near-IR *in* 154  
*vivo*. 155

In contrast to the mid-IR, near-IR spectrometry is 156  
characterized by low molar absorptivities and broad 157  
overlapping bands. *In vivo* vibrational spectrometry has 158  
been plagued historically by problems with high water 159  
absorbance in tissue, light scattering, peak overlap, and peak 160  
shifting with temperature and sample-matrix composition. 161  
The intense absorbance of water more than any other factor 162  
prevents the use of mid-IR spectrometry as a catheter-based 163

164 diagnostic tool in atherosclerosis. Instead, near-IR spectro-  
165 metry has been driven into increasingly complex biological  
166 and medical problems as more intense and more stable light  
167 sources as well as more efficient detectors (and in many  
168 cases, more efficient imaging detectors) have been devel-  
169 oped. Improved methods of obtaining rapid wavelength  
170 selectivity using tunable lasers [10] and integrated sensing  
171 and processing using molecular factor filters [11] are also  
172 playing an important role in advancing near-IR spectrometry  
173 in a clinical setting.

174 Synchrotron infrared light is approximately 1000 times  
175 more intense than a conventional infrared source. In  
176 addition, synchrotron infrared light is highly collimated  
177 like a laser, making it more easily focused onto a small spot.  
178 However, unlike a laser, the synchrotron emits a wide range  
179 of infrared wavelengths, enabling FTIR microspectroscopy.  
180 Consequently, with synchrotron infrared light, samples can  
181 be studied that are smaller and/or more dilute in  
182 concentration. In addition, the 1000-fold increase in  
183 brightness translates to data collection times that are about  
184 30 times faster with the synchrotron source in comparison to  
185 a global source. For this study, use of intense synchrotron  
186 radiation permits small microscopic apertures near the  
187 diffraction limit of the light to be used in microspectrometry,  
188 increasing the spatial resolution of collagens and elastin  
189 attainable at the site of plaque rupture. Measuring IR  
190 fundamentals provides stronger signals with less peak  
191 overlap than available with NIR overtone and combination  
192 bands.

193 Infrared spectrometry has been employed a number of  
194 times in the analysis of arterial collagens and elastin. Human  
195 arterial tissue has been characterized using FT-IR micro-  
196 spectroscopy and chemometrics [12,13]. Comparative  
197 studies of plaques and proteins using FTIR and other  
198 methods have been performed [14]. Collagen modifications  
199 and surface properties of arteries have been studied in a  
200 bovine model<sup>15</sup>. The effect of elastin on the calcification of  
201 collagen–elastin matrix systems has been studied with  
202 infrared spectrometry [16]. Finally, fundamental vibrational  
203 information on collagens and elastin has been derived from  
204 studies using FT-Raman spectrometry [13,17].

205 Similar composition changes have been observed in both  
206 the fibrous cap of lesions in atherosclerosis and in the media  
207 and adventitia of AAAs, albeit on different physical scales  
208 [15,18,19]. Near-infrared spectrometry, immunohistochem-  
209 istry, and scanning electron microscopy with morphometry  
210 have been employed in these studies of collagen and elastin  
211 composition changes. The spectrometric correlation meth-  
212 odology employed in the following study relies on collagen  
213 and elastin content changing within the samples as  
214 suggested by previous research. This preliminary study  
215 tests the hypothesis that the changes observed previously in  
216 collagen I, III, and elastin in aneurysm on a millimeter scale  
217 are similar to the changes that occur in the fibrous cap of  
218 vulnerable atherosclerotic plaque on a scale of micrometers  
219 or tens of micrometers. If successfully demonstrated, the

similarities could be used as in vivo markers of the  
vulnerable plaques most in need of treatment, and could be  
used in monitoring therapies in atherosclerotic plaques  
treated by drugs.

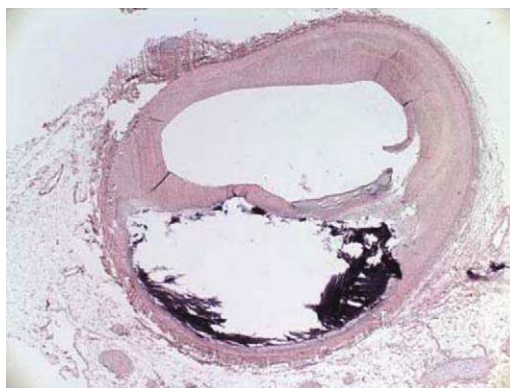
## 2. Experimental

### 2.1. Tissue samples

220 Twenty human coronary tissue sections were obtained  
221 post-mortem without identifiers from a single patient  
222 through the University of Kentucky Medical Center, Clinical  
223 Pathology Services. The study was approved by the  
224 University of Kentucky IRB and HIPAA compliance office.  
225 If components other than collagen and elastin were in the  
226 tissue and were varying in concentration, then the  
227 correlation maps produced by IR imaging would be biased  
228 and would not likely reflect the individual contributions  
229 from collagen I, III and elastin in the sample. The potential  
230 for bias was eliminated by removing all other components of  
231 the tissue visible on IR spectra by a washing, solvent-  
232 extraction and formalin-fixing process prior to mounting the  
233 tissue sections on the slides<sup>7</sup>. The tissue sections were  
234 mounted in paraffin onto two low-e glass slides (SensIR) for  
235 infrared microspectrometry. A visible light image of a  
236 stained section of human coronary atherosclerotic plaque  
237 appears in Fig. 1. This section was adjacent to the section  
238 used for IR microspectrometric imaging (see Fig. 2). An  
239 arrow marks the location on the fibrous cap from which  
240 infrared spectra were obtained. Fig. 3 depicts representative  
241 spectra from a small area of the fibrous cap. A total of 80,600  
242 spectra were obtained from all plaque sections.

### 2.2. Instrumentation

243 The infrared microspectrometer used at beamline U2b of  
244 the vacuum ultraviolet (VUV) storage ring of the National  
245 Synchrotron Light Source (NSLS) at Brookhaven National  
246 Laboratory (BNL), Upton NY consisted of a Nic PLAN<sup>®</sup>  
247



248 Fig. 1. Stained section of human coronary vulnerable atherosclerotic  
249 plaque, obtained as a visible light image. This section was adjacent to  
250 the one used for IR microspectrometric imaging.

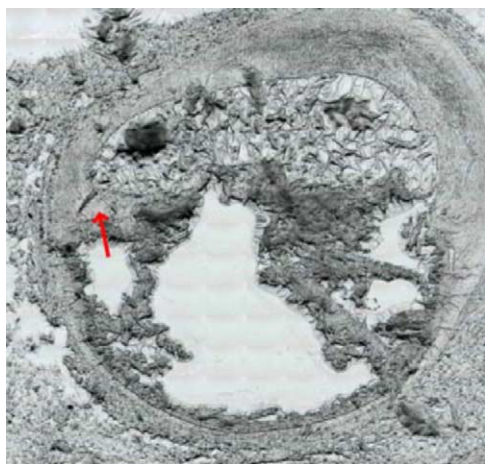


Fig. 2. Unstained section of human coronary vulnerable atherosclerotic plaque, mounted in paraffin. Arrow marks location on fibrous cap from which IR spectra were obtained. This section was adjacent to the section stained and imaged in the visible region. The control image section was at the bottom of the vessel, away from the fibrous cap.

254 infrared microscope interfaced to a Nicolet Magna<sup>®</sup> 860  
255 infrared spectrometer (Thermo Electron, Madison WI). A  
256 liquid nitrogen cooled 250 cm MCT detector that had  
257 maximum signal intensity at 1250  $\mu\text{m}$  was used.

258 Schwartzchild 32 $\times$  and 10 $\times$  all reflecting mirror lenses  
259 were used for the objective and condenser, respectively. A  
260 remote projected image plane mask before the objective  
261 produced the apertures used for single point spectra or raster  
262 scan mapping via a digitally controlled motorized micro-  
263 scope stage. Spectra were recorded in a reflection absorption  
264 mode. A clear location on the infrared reflecting microscope  
265

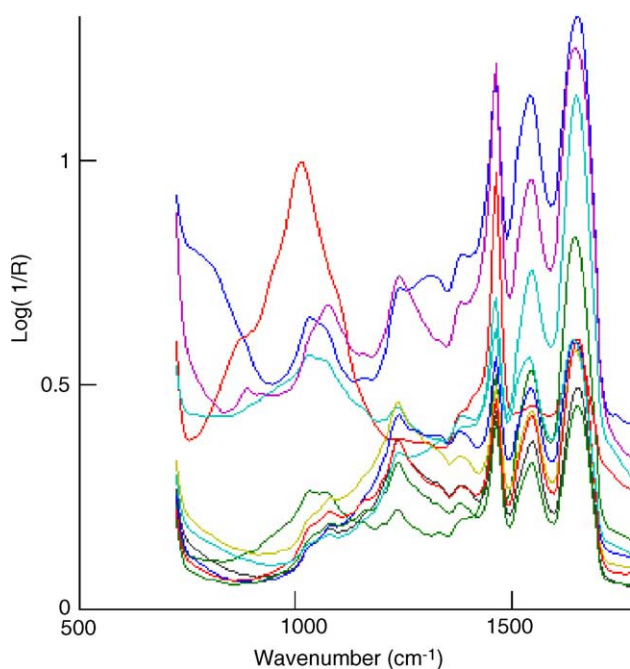


Fig. 3. Representative infrared spectra from the region near the arrow in Fig. 2. The sharp peak at  $1469\text{ cm}^{-1}$  arises from paraffin.

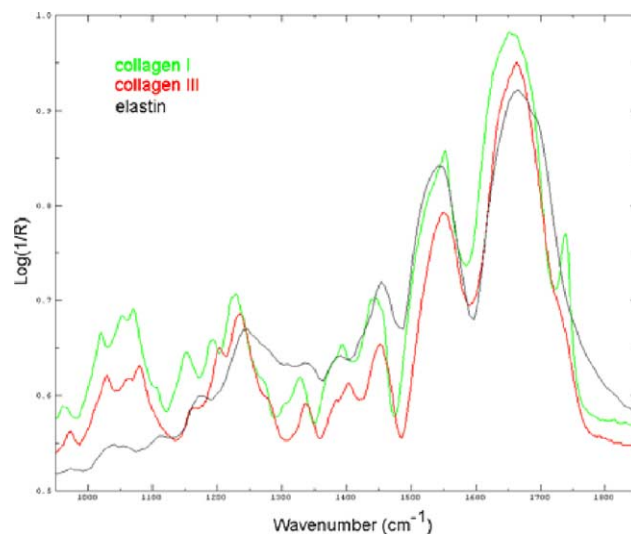


Fig. 4. Spectra of lyophilized standards of collagen I, III, and elastin.

265 slide ReflectIR<sup>®</sup> (SensIR, Danbury CT) was used to obtain a  
266 reflection background spectrum.

267 Mapping was also accomplished from a global source  
268 focal plane array instrument. The Perkin-Elmer Spotlight  
269 model 300 was used to obtain rectangular maps of select  
270 regions of the sections being examined. For focal plane array  
271 images, the  $6.25\ \mu\text{m} \times 6.25\ \mu\text{m}$  pixel size was used.

272 Preliminary examination of each map was done from a  
273 locally baseline corrected peak area for the triplet at  
274  $1236\text{ cm}^{-1}$  and the doublet associated with the  $1082\text{ cm}^{-1}$   
275 band. A map of the ratio of the area of the  $1236\text{ cm}^{-1}$  band to  
276 that of the  $1082\text{ cm}^{-1}$  was used to locate the region with the  
277 highest relative amount of the collagen I.

278 Reference FTIR spectra of collagens I, III, and elastin  
279 (Sigma) were obtained (see Fig. 4). While such reference

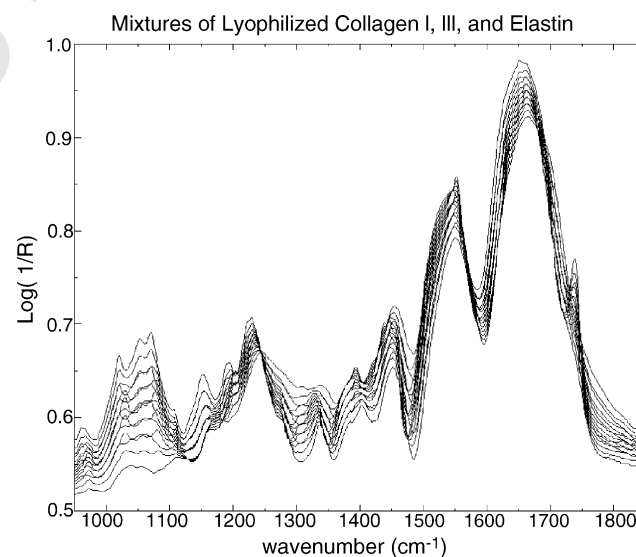


Fig. 5. Spectra of standard mixtures of collagen I, III, and elastin used for mean-centered correlation analysis.

280 compounds are sometimes contaminated by small amounts  
 281 of lipid, potential contamination posed no problem for this  
 282 research because the lipid regions of the spectrum were not  
 283 used in the analysis to avoid the paraffin. The spectral data  
 284 were scatter-corrected prior to data analysis (see Fig. 5).  
 285 Representative spectra from a human coronary tissue section  
 286 are presented in Fig. 3 for comparison with Fig. 5. The sharp  
 287 peak at  $1469\text{ cm}^{-1}$  in Fig. 3 arises from paraffin. The  
 288 chemical composition of the tissue samples between  
 289 adjacent areas of tissue is typically similar, and as a result,  
 290 the gross appearances of the spectra are similar.

291 SEM morphometry provided the reference method for  
 292 collagens and elastin [20]. A contract laboratory (Industrial  
 293 Analytical Services, Leominster, MA) was used to blind the  
 294 spectroscopists and electron microscopists examining the  
 295 tissue sections. A similar methodology was employed by the  
 296 authors in a previous near-IR study of aneurysm6.

### 297 2.3. Data analysis

298 Analytical software was written in Matlab 6.5 (The Math  
 299 Works, Inc., Natick, Mass.). In an effort to determine which  
 300 spectral changes in the coronary sections were associated  
 301 with collagens I and III and elastin composition changes, a  
 302 set of sample mixtures of collagens I and III and elastin was  
 303 prepared using pure lyophilized standards (see Fig. 5). A  
 304 triangular array of compositions was constructed for this  
 305 study similar to the one used in Ref. [6]. The composition of  
 306 each of the prepared sample standards was represented by a  
 307 vertex in the array, with the pure collagen I (C1) standard in  
 308 one corner of the triangle, the pure collagen III (C3) in  
 309 another corner of the triangle, and finally the pure elastin in  
 310 the remaining corner of the triangle. The concentrations of  
 311 each constituent in the standard mixtures were set at 0, 25,  
 312 50, 75, or 100 wt.% of each lyophilized protein. The  
 313 vertexes represent all possible combinations of mixtures in  
 314 the percentages given (a total of 15 mixtures including the  
 315 pure corner standards). The center (i.e., group mean) would  
 316 represent a mixture of one-third of each protein, but this

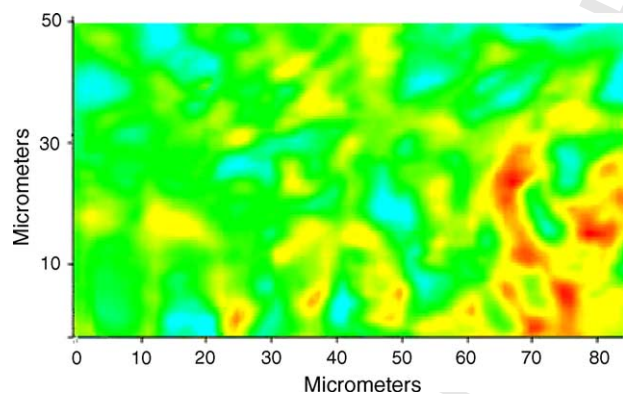


Fig. 6. Collagen I distribution in targeted region of fibrous cap (red = high, blue = low concentration). (For interpretation of the references to color in this figure legend, the reader is referred to the web version of the article.)

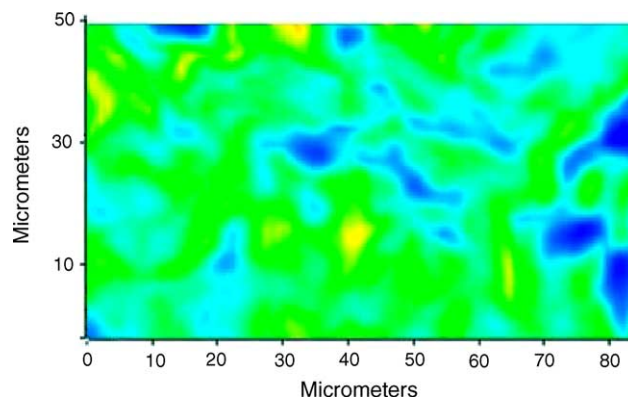


Fig. 7. Collagen III distribution in targeted region of fibrous cap (yellow = high, blue = low concentration). (For interpretation of the references to color in this figure legend, the reader is referred to the web version of the article.)

317 sample was not actually prepared in the set. The reflection  
 318 spectra of the 15 mixtures were compared to the reflection  
 319 spectra of the coronary sections by mean-centering the  
 320 spectra of the mixtures and the spectra of the coronary artery  
 321 sections. The difference spectra between each standard  
 322 sample spectrum and the mean spectrum of the standard  
 323 samples were calculated. Likewise, the difference spectra  
 324 between each coronary section spectrum and the mean  
 325 spectrum of the coronary sections were also calculated.  
 326 Finally, the difference spectra of the standards and the  
 327 coronary sections were then correlated using the product-  
 328 moment correlation coefficient. The values of these  
 329 correlation coefficients were contour plotted to produce  
 330 images corresponding to collagen I, III, and elastin in  
 331 Figs. 6–9.

### 3. Results and discussion

332 The correlations between the coronary tissue section  
 333 spectra and the set of standard sample spectra ranged  
 334 between  $\pm 0.99$ . In consequence, the contours in Figs. 6–8  
 335 covered a wide range of correlation values (as did the pixels  
 336

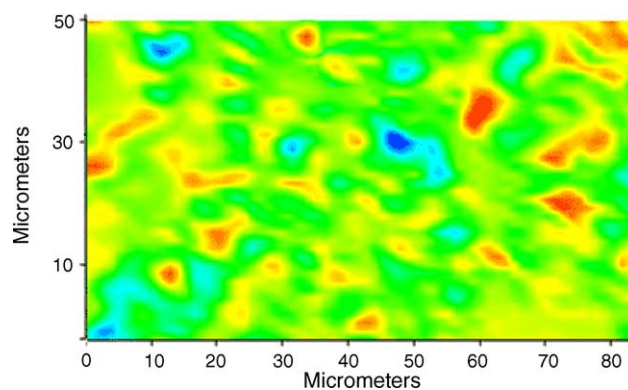


Fig. 8. Elastin distribution in targeted region of fibrous cap (red = high, blue = low concentration). (For interpretation of the references to color in this figure legend, the reader is referred to the web version of the article.)

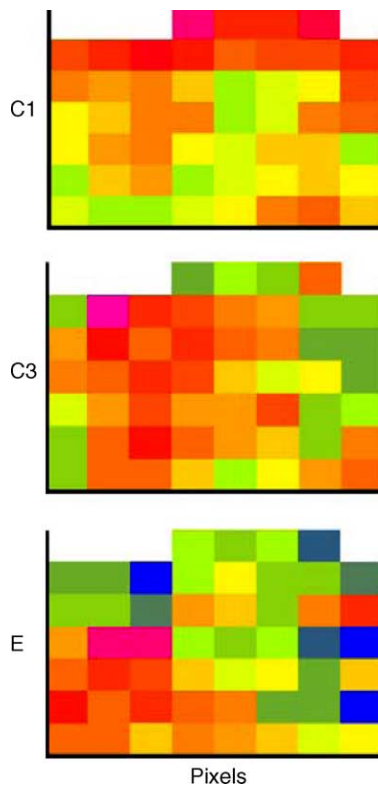


Fig. 9. Localized distribution of collagen I, collagen III, and elastin at individual pixel resolution.

in Fig. 9). Color was used to represent correlation between the spectra of the coronary sections and reference standards. Violet represents the lowest correlation, while red represents the highest. The region at the far left of Figs. 6–8, off the edge of the thin cap, served as a sort of internal standard or control for the images as the scanning progressed toward the right and the thinnest portion of the cap.

Fig. 6 shows the correlation between the tissue spectra and amount of collagen I in the standards in the region marked by the arrow in Fig. 2. Pixel values were interpolated between the concentrations of the standards to reach the maximum correlation, as performed in Ref. [6]. While the amount of collagen I does not increase monotonically from left to right in the image, there is a gradient in concentration over the 80  $\mu\text{m}$  distance across the fibrous cap. The right side of the image in Fig. 6 is the side closest to the thinnest area of the fibrous cap, as shown in Fig. 1.

Fig. 7 depicts the distribution of collagen III predicted in a similar manner. Collagen III also shows an overall gradient, but instead generally decreases nonmonotonically from left to right in the image. In contrast, the amount of elastin did not appear to change substantially across the field of the image (see Fig. 8). However, most of the loss of elastin could have occurred long before the coronary tissue was collected. The control section imaged at the bottom of the vessel was similar to Fig. 8 in that it showed no obvious concentration trends for either the collagens or elastin. Overall, the trends in collagen I, III, and elastin observed in

human coronary plaque are similar to those observed in AAA. At single pixel resolution on the right side of the sample zone nearest the thinnest region of the fibrous cap (see Fig. 9), gradients are not as clear.

Rupture-prone plaques are not the lone vulnerable plaques. All categories of atherosclerotic plaques with high probability of thrombotic complications and swift progression should be regarded as vulnerable plaques. Furthermore, vulnerable plaques are not the only culprit features leading to the occurrence of acute coronary syndromes, myocardial infarction, and sudden cardiac death. Vulnerable blood (i.e., blood inclined toward thrombosis) and vulnerable myocardium (inclined toward lethal arrhythmia) perform an essential role in the clinical outcome. The phrase “vulnerable patient” has even been proposed for the classification of persons with high probability of emergent cardiac events in the near future. A quantitative means of cumulative risk assessment of vulnerable patients should be created that includes variables describing plaque, blood, and myocardial vulnerability. Newly developed assays (e.g., for C-reactive protein), imaging techniques (e.g., CT and MRI), non-invasive electrophysiological tests (for vulnerable myocardium), and promising catheters (to localize and characterize vulnerable plaque), together with prospective genomic and proteomic methods, will lead researchers in the hunt for vulnerable patients. These analytical methods will also lead to the expansion and exploitation of new therapies, and eventually to reduction in the incidence of acute coronary syndromes and sudden cardiac death.

This preliminary study has some important limitations. A single patient served as the source of the 80,600 spectra collected from 24 coronary sections, limiting the observable variation in the data set. The lack of detailed histological data for the samples and lack of clinical history from the patient prevents the association of the spectra with specific tissue pathologies and comparison of pathology. Most importantly, the exact location of any rupture (the culprit lesion) was not uncovered in the tissue sections. For this reason, the exact nature of the gradients within 10  $\mu\text{m}$  of any tear in the fibrous cap cannot be determined. However, the fact that gradients in collagen and elastin similar to those observed in AAAs do exist in the vicinity of a plaque rupture suggests that similar mechanisms of protein degradation may be responsible in both disease states. Thus, an increase in collagen I at the expense of collagen III (and possibly of elastin) might serve as a marker of plaques needing an immediate intervention.

#### 4. Conclusion

Like near-IR spectra, mid-IR spectra are distinctive for proteins in the blood vessel wall (specifically collagens and elastin). The results of this preliminary study suggest that synchrotron IR microspectroscopy is a potentially useful technique for investigating vascular changes and protein

418 composition associated with cardiovascular disease. In  
 419 particular, synchrotron IR microspectroscopy has the light  
 420 intensity, and thus spatial resolution using small mask  
 421 apertures, needed to quantify collagens and elastin within  
 422 10  $\mu\text{m}$  of the site of plaque rupture. These early results  
 423 support an expanded study in the future employing IR  
 424 spectra to characterize completely chemical compositions  
 425 within 10  $\mu\text{m}$  of the location of plaque rupture. If the  
 426 compositions of many of these small regions prove similar in  
 427 many different patients, a useful marker will have been  
 428 demonstrated that can be targeted by near-IR catheters in  
 429 vivo.

### 430 Acknowledgment

431 This work was supported in part by KSEF-148-502-03-61  
 432 and by the Kansas State University Microbeam Spectro-  
 433 scopy Laboratory. The research was carried out in part at the  
 434 National Synchrotron Light Source, Brookhaven National  
 435 Laboratory, which is supported by the U.S. Department of  
 436 Energy, Division of Materials Sciences and Division of  
 437 Chemical Sciences, under Contract No. DE-AC02-  
 438 98CH10886. The work could not have been performed  
 439 without the invaluable technical assistance of Tiffany Fisher  
 440 (KSU), Nebojsa Marinkovic (NSLS), and Randy Smith  
 441 (NSLS).

### 442 References

- 443 [1] M. Naghavi, P. Libby, E. Falk, S.W. Casscells, S. Litovsky, R.A.  
 444 Lodder, P.K. Shah, J.T. Willerson, From vulnerable plaque to vulner-  
 445 able patient: a call for new definitions, *Circulation* 108 (14) (2003)  
 446 1664–1672.
- 447 [2] F.D. Kolodgie, A.P. Burke, A. Farb, et al. The thin-cap fibroatheroma:  
 448 a type of vulnerable plaque: the major precursor lesion to acute  
 449 coronary syndromes, *Curr. Opin. Cardiol.* 16 (2001) 285–292.
- 450 [3] R.W. Wissler, J.P. Strong, Risk factors and progression of athero-  
 451 sclerosis in youth. PDAY Research Group. Pathological determinants  
 452 of atherosclerosis in youth, *Am. J. Pathol.* 153 (1998) 1023–1033.
- 453 [4] E.M. Tuzcu, S.R. Kapadia, E. Tutar, et al. High prevalence of coronary  
 454 atherosclerosis in asymptomatic teenagers and young adults: evidence  
 455 from intravascular ultrasound, *Circulation* 103 (2001) 2705–2710.
- 456 [5] G. Pasterkamp, A.H. Schoneveld, A.C. van der Wal, et al. Relation of  
 457 arterial geometry to luminal narrowing and histologic markers for

- plaque vulnerability: the remodeling paradox, *J. Am. Coll. Cardiol.* 32  
 (1998) 655–662. 458
- [6] A. Urbas, M.W. Manning, A. Daugherty, L.A. Cassis, R.A. Lodder,  
 Near-infrared spectrometry of abdominal aortic aneurysm in the ApoE  
 –/– mouse, *Anal. Chem.* 75 (14) (2003) 3650–3655. 459  
 460  
 461  
 462
- [7] P.R. Moreno, R.A. Lodder, K.R. Purushothaman, W.E. Charash, W.N.  
 O'Connor, J.E. Muller, Detection of lipid pool, thin fibrous cap, and  
 inflammatory cells in human aortic atherosclerotic plaques by near-  
 infrared spectroscopy, *Circulation* 105 (8) (2002) 923–927. 463  
 464  
 465  
 466
- [8] L.A. Cassis, R.A. Lodder, *Anal. Chem.* 65 (9) (1993) 1247–1256. 467
- [9] R.J. Dempsey, R.A. Lodder, *Ann. N. Y. Acad. Sci.* 820 (1997) 149–  
 169. 468  
 469
- [10] L.A. Cassis, W.C. Symons, R.A. Lodder, Cardiovascular near-infrared  
 imaging, *J. Near-Infrared Spectrom.* 6 (1998) A21–A25. 470  
 471
- [11] L.A. Cassis, A. Urbas, R.A. Lodder, Hyperspectral integrated com-  
 putational imaging, *Anal. Bioanal. Chem.* (2004)10.1007/s00216-  
 004-1. 472  
 473  
 474
- [12] J.M. Gentner, E. Wentrup-Byrne, P.J. Walker, M.D. Walsh, Compar-  
 ison of fresh and post-mortem human arterial tissue: an analysis using  
 FT-IR microspectroscopy and chemometrics, *Cell Mol. Biol. (Noisy-  
 le-grand)* 44 (1) (1998) 251–259. 475  
 476  
 477  
 478
- [13] R. Manoharan, J.J. Baraga, R.P. Rava, R.R. Dasari, M. Fitzmaurice,  
 M.S. Feld, Biochemical analysis and mapping of atherosclerotic  
 human artery using FT-IR microspectroscopy, *Atherosclerosis* 103  
 (2) (1993) 181–193. 479  
 480  
 481  
 482
- [14] A. Becker, M. Epple, K.M. uller, I. Schmitz, A comparative study of  
 clinically well-characterized human atherosclerotic plaques with his-  
 tological, chemical, and ultrastructural methods, *J. Inorg. Biochem.* 98  
 (12) (2004) 2032–2038. 483  
 484  
 485  
 486
- [15] E. Wang, K. Thyagarajan, R. Tu, D. Lin, C. Hata, S.H. Shen, R.C.  
 Quijano, Evaluation of collagen modification and surface properties of  
 a bovine artery via polyepoxy compound fixation, *Int. J. Artif. Organs*  
 16 (7) (1993) 530–536. 487  
 488  
 489  
 490
- [16] A. Singla, C.H. Lee, Effect of elastin on the calcification rate of  
 collagen-elastin matrix systems, *J. Biomed. Mater. Res.* 60 (3) (2002)  
 368–374. 491  
 492  
 493
- [17] L. Silveira Jr., S. Sathaiiah, R.A. Zangaro, M.T. Pacheco, M.C.  
 Chavantes, C.A. Pasqualucci, Near-infrared Raman spectroscopy of  
 human coronary arteries: histopathological classification based on  
 Mahalanobis distance, *J. Clin. Laser Med. Surg.* 21 (4) (2003)  
 203–208. 494  
 495  
 496  
 497  
 498
- [18] A. Daugherty, M.W. Manning, L.A. Cassis, Angiotensin II promotes  
 atherosclerotic lesions and aneurysms in apolipoprotein E-deficient  
 mice, *J. Clin. Invest.* 105 (2000) 1605–1612. 499  
 500  
 501
- [19] V. Neumeister, M. Scheibe, P. Lattke, W. Jaross, Determination of the  
 cholesterol-collagen ratio of arterial atherosclerotic plaques using near  
 infrared spectroscopy as a possible measure of plaque stability,  
*Atherosclerosis* 165 (2) (2002) 251–257. 502  
 503  
 504  
 505
- [20] A.M. Sharifi, J.S. Li, D. Endemeann, E.L. Schiffrin, Effects of  
 enalapril and amlodipine on small-artery structure and composition,  
 and on endothelial dysfunction in spontaneously hypertensive rats, *J.*  
*Hypertension* 4 (1998) 457–466. 506  
 507  
 508  
 509

510

UNCORRECTED